Distribution Agreement

In presenting this thesis as a partial fulfillment of the requirements for a degree from Emory University, I hereby grant to Emory University and its agents the non-exclusive license to archive, make accessible, and display my thesis in whole or in part in all forms of media, now or hereafter now, including display on the World Wide Web. I understand that I may select some access restrictions as part of the online submission of this thesis. I retain all ownership rights to the copyright of the thesis. I also retain the right to use in future works (such as articles or books) all or part of this thesis.

Mandy Chan April 12, 2018

Prion Delivery via Peptide-Nucleic Acid Co-assembly: the Inside-out Virus

by

Mandy Chan

David Lynn
Adviser

Department of Chemistry

David Lynn

Adviser

Younggang Ke

Committee Member

Arri Eisen

Committee Member

2018

Prion Delivery via Peptide-Nucleic Acid Co-assembly: the Inside-out Virus

By

Mandy Chan

David Lynn

Adviser

An abstract of
a thesis submitted to the Faculty of Emory College of Arts and Sciences
of Emory University in partial fulfillment
of the requirements of the degree of
Bachelor of Sciences with Honors

Department of Chemistry

2018

Abstract

Prion Delivery via Peptide-Nucleic Acid Co-assembly: the Inside-out Virus
By Mandy Chan

Protein-nucleic acid interaction drives the chemical evolution of life as well as the pathogenesis of neurodegenerative diseases. In order to better understand this interaction between these two important biopolymers, we aimed to develop an inside-out virus that reverses the normal viral architecture and functions of protein and nucleic acid. Such a virus would deliver information stored in proteins using nucleic acids as a vehicle for cellular uptake. Here we provide the preliminary results of the construction of a fluorescent peptide-DNA co-assembly and its cellular internalization performance. Fluorophore-tagged, prion-like amyloid-β peptide and single-stranded DNA were co-assembled to achieve a PBS-stable, heterogeneous system with nanotubes and fibers. Dilution of the tagged-DNA as an initial attempt to resolve the heterogeneity yielded interesting results as maturing ribbons were replaced by bundled fibers. Flow cytometry on assembled peptide-treated non-small lung cancer cell lines showed that peptide fibers did not associate with cells. Meanwhile, confocal micrographs demonstrated the stability, co-localization of components, and preferential attachment of the co-assemblies to cells.

Prion Delivery via Peptide-Nucleic Acid Co-assembly: the Inside-out Virus

By

Mandy Chan

David Lynn

Adviser

A thesis submitted to the Faculty of Emory College of Arts and Sciences
of Emory University in partial fulfillment
of the requirements of the degree of
Bachelor of Sciences with Honors

Department of Chemistry

2018

Acknowledgements

I would like to thank my research advisor Dr. David Lynn for his generous support, and mentorship throughout my time in the lab. He has pushed me to reach higher, to think outside of the box, and to be persistent. I am extremely thankful for his dedication to train young scientists and his inspiration for me to pursue a graduate degree.

Every past and current member of the Lynn lab has also provided me tremendous support in every step of my research project and I greatly appreciate every single of them: Dr. Olga Taran, Dr. Yushi Bai, Dr. Allisandra Rha, Dr. Chen Liang, Dr. Rolando Rengifo, Dr. Jackey Hsieh, Noel Li, Anthony Sementilli, Siying Cen, Youngsun Kim, Christella Dhammaputri, Lucy Eum, Chad Hicks, Ronnie Festok, and Anirudh Pidugu. Particularly, I want to say thank you for Anthony Sementilli for his excellent mentorship as my graduate student mentor since my first day in lab.

The cell assay portion of this project would not have been possible without the support of my collaborators Dr. Pengfei Wang in the Ke lab and Dr. Mohammad Aminur Rahman in the Shin lab. I would like to thank them for their consultation, experimentation, and support.

Finally, I am very thankful for my committee member, Dr. Yonggang Ke, and Dr. Arri Eisen for providing thought-provoking questions to move my research project forward and for serving on my committee.

Table of Contents

Introduction

The interaction between proteins and nucleic acids, the two major biopolymers that drive information flow in living systems, is critical for the exploration of prebiotic chemical events that resulted in the emergence of life. The initial focus, however, has been placed on nucleic acid as the RNA world hypothesis is proposed to explain the preceding events leading to the central dogma. This hypothesis is driven by RNA's potential to store genetic information and perform as a catalyst in primitive cells[1]. While the discovery of ribozymes[2] further validates this hypothesis, the ribosome, an important exemplifier of a ribozymes, relies heavily on the mutualistic balance between protein's structural support and RNA's catalytic activities[3]. The resulting translation is the product of this protein/nucleic acid cooperation in the ribosome[4].

Although nucleic acids are an integral part in the evolution of life, especially for its capability of information storage and transfer, proteins have recently challenged nucleic acids as the only carrier of information in evolution[5-6]. Prions are self-propagating protein entities that form cross-β amyloid aggregates with various morphologies[7-8]. Most interestingly, a prion can infect normal cellular protein isoforms, converting them into a misfolded, infectious prion isoform. Furthermore, because of its infectious nature and its location in the cytoplasm, cytoduction, which is cell division that yields mixed cytoplasm but nucleus of one parent, in yeast effectively allows the meiotic progeny to inherit the dominant prion traits[5, 7, 9]. This protein-only hypothesis stands out as an exception to the common flow of information utilizing nucleic acid[9-11].

In addition to the newly discovered role of proteins in informational transfer, nucleic acids also interact with proteins to facilitate stabilization, particularly in the context of neurodegenerative diseases such as prion disease and Alzheimer's Disease (AD). Single-stranded

RNA has been shown to be a cellular cofactor to stimulate the conversion of normal prion protein to infectious agent; nonspecific DNA also gives rise to different secondary and tertiary structures in prion aggregates which have distinct level of cytotoxicity[12-14]. Meanwhile, AD-associated amyloid-β (Aβ) can also self-replicate and assemble in an environment-dependent fashion to form diverse morphologies [15-16]. Notably, it has been reported that charged phosphate backbone of nucleic acids catalyzes the formation of amyloid fibrils, and in turn, amyloid organizes nucleic acids and promotes hybridization[17].

Given these discoveries, we intended to explore the idea of protein carrying information and to better understand protein-nucleic acid interaction in the context of AD[18]. Specifically, recent study of the effective cellular endocytosis of DNA nanorod constructed by DNA origami technique[19-20] inspired the design of an inside-out virus. While traditional viral architecture utilizes the protein capsule to protect and deliver the viral genome, we wanted to determine whether nucleic acids in an inside-out virus might stabilize and deliver an infectious prion-like protein. Given the ability of DNA nanostructure to cross cell membranes effectively, we hypothesize that the inside-out virus will increase the degree of cellular uptake of the Aβ peptide to promote intracellular protein aggregation.

To construct a prototype of this inside-out virus, we turned to the prion-like Aβ peptide. Aβ peptide is advantageous for it is well-characterized and relevant to AD [21-22]. Numerous studies have characterized the peptide's structure, self-assembling capability, sensitivity to environment, [15-16, 21, 23-25]. The Aβ canonical nucleating core, KLVFFAE, is a simplified amyloid system that also self-assembles into different morphologies. Various manipulation of this nucleating core has led to development of peptide frameworks that can catalyze chemical reaction [26], incorporate photo-redox materials [27], and construct asymmetric bilayer membrane[28].

Particularly, a mutated Aβ nucleating core has been shown to be able to interact with nucleic acid in a stable fashion. With phenylalanine replaced with isoleucine and glutamic acid replaced with glycine, peptide Ac-KLVIIAG-NH_2 co-assembles with nucleic acid to form robust, multilamellar nanotube structures via electrostatic forces between positively charged lysine and negatively charged phosphate backbone (Rha, submitted). While electrostatic force microscopy locates nucleic acid on the outside of these structures, destruction of co-assembly with nuclease demonstrated the impact of nucleic acid to the integrity of the structure as well as its accessibility to the environment (Rha, submitted).

To test the level of cellular association of this inside-out virus prototype, attachment of fluorophores on the peptide[29] and nucleic acid permits tracking of the co-assembly and its biopolymer components with respect to cells. Here we report the progress toward the optimization and characterization of the fluorophore-tagged co-assembly and initial assessment of its cellular association by transmission electron microscopy and confocal microscopy.

This initial construction of the inside-out virus via various approaches do not only test the plasticity of these biological materials, but also serve to elucidate protein-nucleic acid interactions in the context of neurodegenerative diseases and the origin of life. Ultimately, the inside-out virus could catalyze the development of novel tools for native protein delivery.

Results and Discussion

Fluorophore-tagged peptide/nucleic acid co-assembly

Previous reports have shown that peptide Ac-KLVIIAG-NH_2 co-assembles with nucleic acid. To generate a fluorescent co-assembly, we attached rhodamine-110 to the N terminus of the peptide in place of the acetyl cap, and another fluorophore Cy3 to the 3' terminus of single-stranded $DNA(A)_{10}$. The two fluorophores have distinct excitation wavelength, permitting tracking of the two biopolymers and quantification of fluorescence.

We first examined the possibility of co-assembling fluorophore-tagged peptide and nucleic acid to achieve similar nanotube morphology as previously reported (Rha, submitted). After assembling desalted and disaggregated rhodamine-tagged peptide (Rho-KLVIIAG-NH_2) (**Figure 1**) and untagged peptide in 1:250 ratio[29], the assembly showed similar Fourier Transform Infrared (FT-IR) profile (**Figure 2**) and morphology of straight fibers (**Figure 3a**) as untagged peptide (Rha, submitted). Hereby, the mixture of rhodamine-tagged and untagged peptide in 1:250 ratio will be referred as Rho-peptide. When the Rho-peptide was co-assembled with Cy3-tagged DNA in a 1:1 charge ratio at 37˚C in 40% acetonitrile, FT-IR profile showed that β-sheet amide I signaled at around 1625 cm^{-1} (**Figure 2**). From Transmission electron microscopy (TEM), the co-assembly exhibited distinct morphology with an intermediate stage of stripped ribbons on day 5 (**Figure 3b**) and subsequent nanotubes on day 21 and beyond (**Figure 3c**). These structures were also observed in previously reported untagged co-assemblies (Rha, submitted). Colored, gel-like co-assemblies were observed after a few hours post-incubation. While the ribbons and nanotubes were similar in morphology with previous report (Rha, submitted), the present co-assembly was heterogeneous as a mixture of nanotubes and bundled fibers was observed (**Figure 3c**).

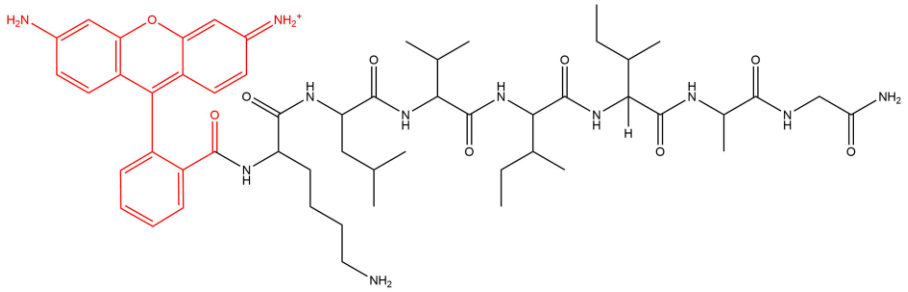

Figure 1. Structure of the rhodamine 110-tagged KLVIIAG-NH_2 peptide.

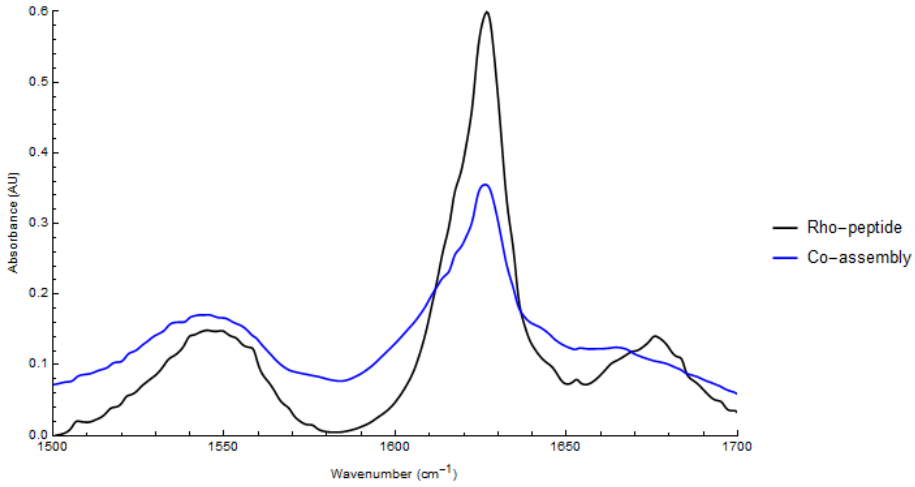

Figure 2. FT-IR profile of Rho-peptide and Rho-peptide/nucleic acid co-assembly showed β-sheet signature signal with the amide I stretch at ~1625 cm^{-1}.

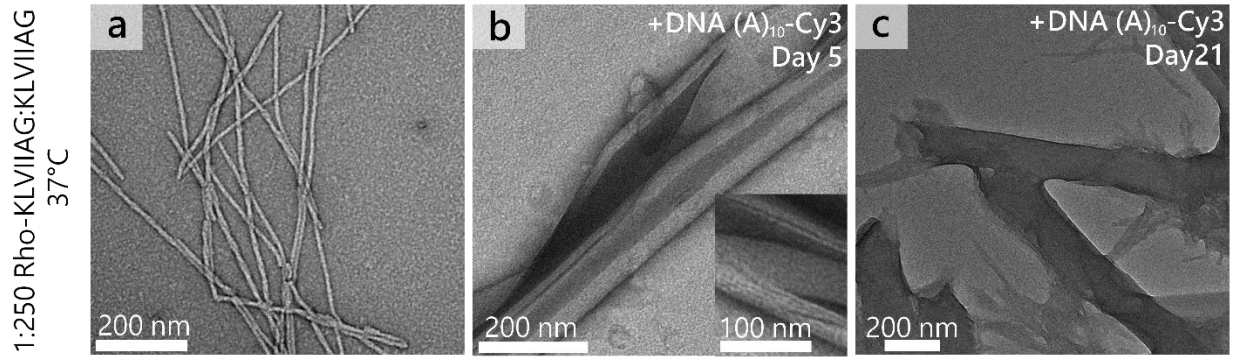

Figure 3. Co-assembly of mixed rhodamine-tagged and untagged peptide with Cy3-tagged DNA formed multilamellar ribbon after day 5 of incubation and nanotube morphologies that are distinct from fibrils formed by peptide alone after 21 days of incubation. These morphologies were consistent with the untagged version. (a) 1:250 Rho-KLVIIAG-NH_2: Ac-KLVIIAG-NH_2 assembly at 37 °C in 40% acetonitrile in water. (b) Day 5 co-assembly of Rho-peptide with Cy3-tagged DNA at 37°C in 40% acetonitrile in water. Inset shows the multilamellar walls of the ribbon. (c) Day 21 co-assembly of Rho-peptide with Cy3-tagged DNA at 37°C in 40% acetonitrile in water.

As the ultimate goal of this project was to test the cellular uptake effectiveness of the co-assembly, the co-assembly's stability in 1X phosphate-buffered saline (PBS) was tested. After centrifugation and removal of organic solvent, the co-assembly was re-suspended in 1x PBS and morphology was observed by TEM. After 5 days at 37°C, the structures in the co-assembly sample remained intact (**Figure 4**).

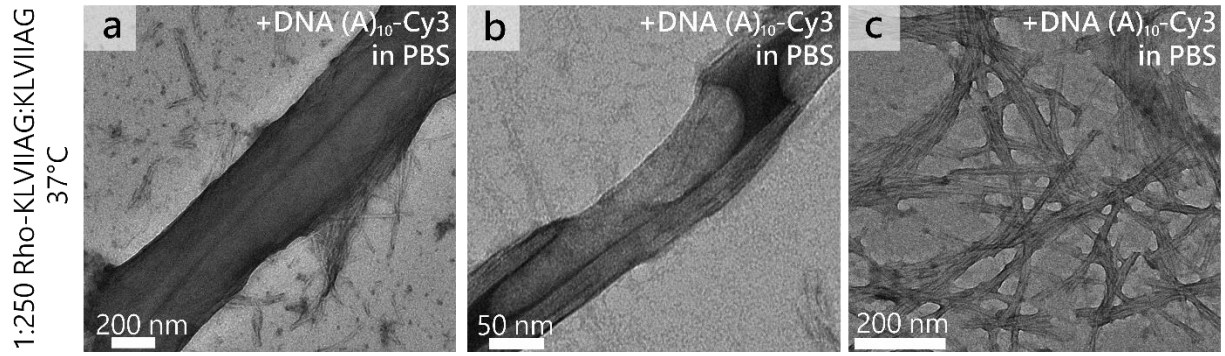

Figure 4. Morphologies of peptide-DNA co-assembly persist after re-suspending in 1X PBS. (a) Mature 1:250 Rho-KLVIIAG-NH_2: Ac-KLVIIAG-NH_2/DNA co-assembly at 37°C in 1x PBS. (b) Maturing co-assembly at 37°C in 1x PBS. Multilamellar walls are visible. (c) Fibers found in co-assembly at 37°C in 1x PBS.

Since the peptide and nucleic acid interact via electrostatic forces, previous report has utilized desalted peptide to eliminate TFA salt that could potentially saturate sites for nucleic acid interaction. However, the desalting step was not optimal for this peptide as it could not provide reliable yield, which varied from 0% to 150 %. Moreover, lyophilization at the end of peptide synthesis is theoretically sufficient to remove most of the TFA salt. Therefore, we attempted to co-assemble peptide with tagged nucleic acid, again in a 1:1 charge ratio, without desalting the peptide. On day 17, the co-assembly without desalting showed comparable nanotubular morphology as its desalted counterpart (**Figure 5**). Since the morphologies of desalted and un-desalted co-assembly were comparable, subsequent experiment utilized un-desalted peptides.

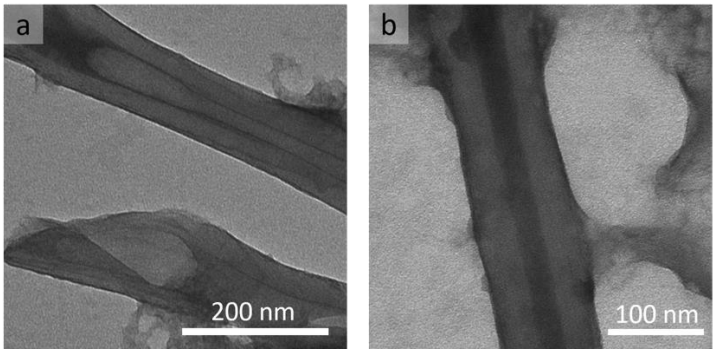

Figure 5. Co-assembly of undesalted peptide with DNA resembled its desalted counterpart. a) Undesalted 1:250 Rho-KLVIIAG-NH_2: Ac-KLVIIAG-NH_2 and Cy3-tagged DNA co-assembly at 37 °C in 40% acetonitrile in water. b) Undesalted Ac-KLVIIAG-NH_2 and Cy3-tagged DNA co-assembly at 37 °C in 40% acetonitrile in water.

Meanwhile, as previous fluorophore-tagged co-assembly produced a heterogeneous system, we hypothesized that the fluorophores can potentially reduce the interaction between peptide and nucleic acid for steric reasons. To test this hypothesis, the ratio of tagged DNA: untagged DNA was altered for co-assembly, while the other perimeters were unchanged. Specifically, we used 1:2, 1:10, and 1:100 ratio of Cy3-tagged DNA: untagged DNA in the co-assembly.

Without the participation of nucleic acid, un-desalted peptide assembled into long, straight fibers similar to its desalted counterpart (**Figure 3a**). For the co-assemblies, pink gel-like precipitates were observed in the first day of incubation, indicating the successful integration of Cy3-DNA with the peptide. During the initial stage of maturation, the co-assemblies for all ratio of tagged DNA produced mostly bundled fibers mixed with ribbons (**Figure 6**). During maturation, more ribbons were produced, and the amount of bundled fibers was reduced (**Figure 6**). After 36 days of incubation, the co-assembly was dominated by bundled fibers (**Figure 6**). There was no difference among co-assemblies with different ratio of tagged: untagged DNA, suggesting that the fluorophores were not obstructing the formation of nanotubes. In fact, this result was surprising since most of the DNAs used in the co-assemblies were untagged. This

observation suggests perhaps the incompatibility of mixing tagged and untagged nucleic acid with tube formation. Further optimization of the system by altering the amino acid sequence of the peptide used for co-assembly and considering other fluorophore options may be necessary. Additionally, the maturation of the co-assembly can also be monitored through circular dichroism. Alternative strategies to form more stable links between peptide and nucleic acid should also be considered. For example, the environment-sensitive, reversible covalent bond of boronic acid with alcohol and amine can be exploited to synthesize boronic acid-functionalized RNA, amino acid, or peptide that can promote the interaction of the two biopolymers with high stability.

Cellular association of Rho-peptide measured by flow cytometry

To assess the peptide's baseline ability to associate with cells, Rho-peptide was assembled in 40% acetonitrile at 37 ˚C, sonicated for 30 seconds, and then re-suspended in 1X PBS (**Figure 7**) before incubation with H1299 non-small lung cancer cells. The lung cancer cell line was used because we intended to compare the internalization effectiveness of the present assemblies with the DNA origami nanostructures, which were incubated with this cell line[19-20]. After incubation for 0.5 and 4 h, no significant change in the percentage of fluorescent cells and intensity of fluorescence were detected relative to control (PBS) (**Figure 8a**). Unassembled Rho-KLVIIAG-NH_2 peptides were also incubated with cells at the same concentration and showed a significant increase of fluorescent cells and intensity (**Figure 8b**). These observations suggest that while smaller, free peptides can potentially cross the cell membrane, peptide assemblies such as the Rho-peptide cannot. Interestingly, while the longest DNA nanostructures were most readily internalized by the lung cancer cells because they interact with more scavenger receptors[20] in comparison with other structures, we observed an opposite trend with the

incubation of peptide assemblies. Future experiments can include further sonication the fibers into smaller pieces and comparison of their cellular association and uptake efficiency with the present study.

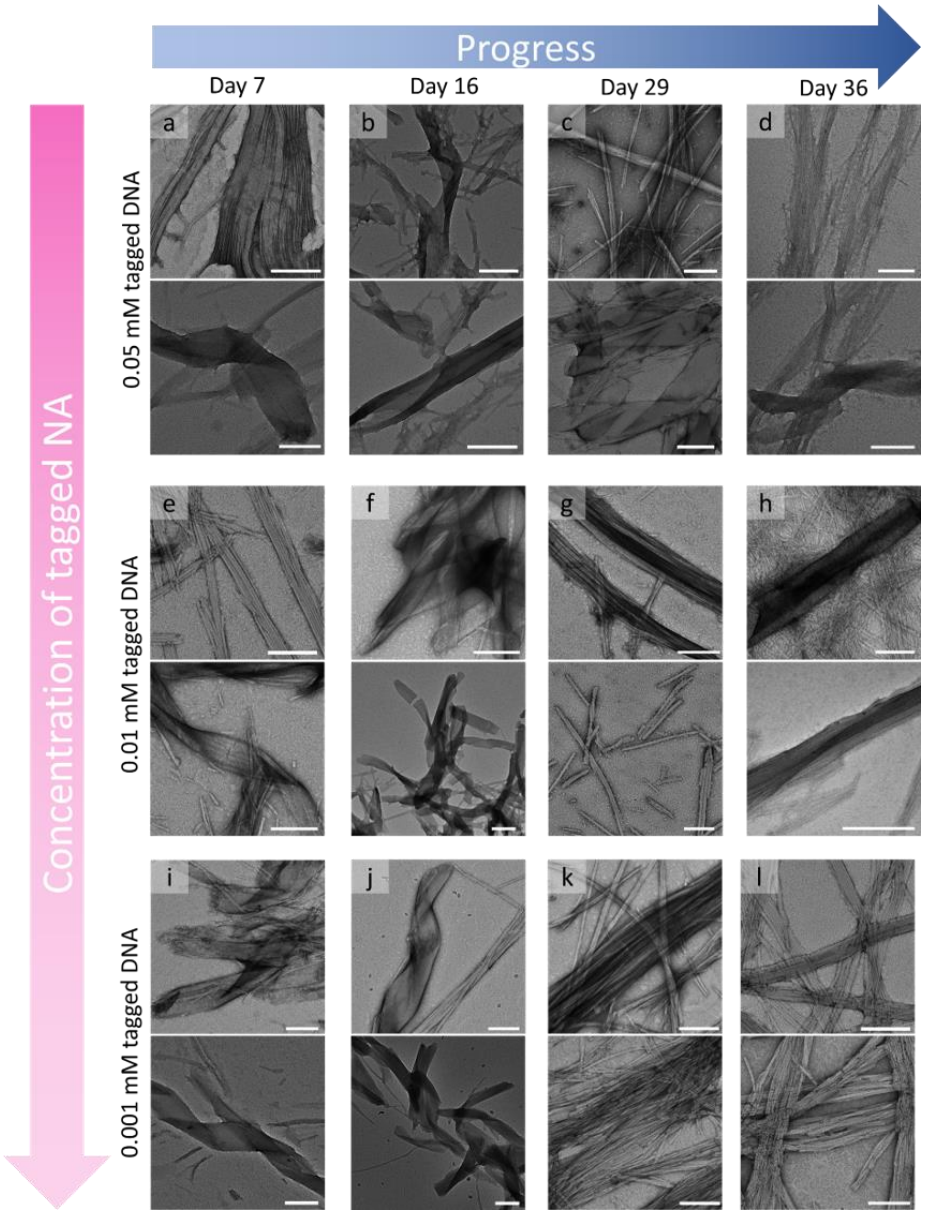

Figure 6. Co-assemblies of 1:250 Rho-KLVIIAG-NH2: Ac-KLVIIAG-NH2 (Rho-peptide) with different ratio of untagged: Cy3-tagged DNA ratio in 40% acetonitrile at 37 ˚C through maturation. Ribbons emerged in the initial stage of co-assembly, but only bundled ribbons were observed after 36 days. a-d) Co-assemblies of Rho- peptide with 1:2 ratio of tagged: untagged DNA. e-h) Co-assemblies of Rho-peptide with 1:10 ratio of tagged: untagged DNA. i-l) Co-assemblies of Rho-peptide with 1:100 ratio of tagged: untagged DNA. Scale bars = 200 nm.

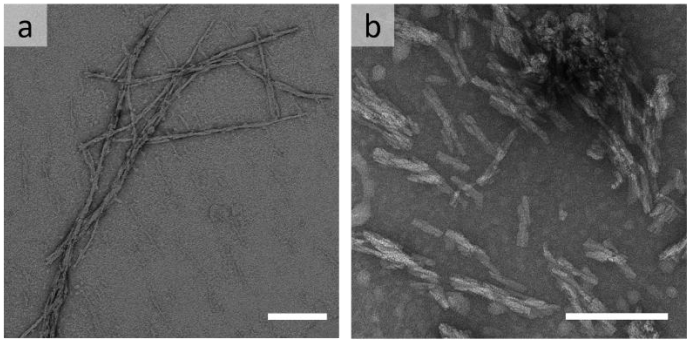

Figure 7. Resuspended, sonicated Rho-peptide fibers maintained stable morphology in 1X PBS before cellular incubation for flow cytometry analysis. a) Rho-peptide formed straight and long fibers. b) Sonicated Rho-peptide fibers were fragmented into various lengths. Scale bar = 200 nm.

Confocal microscopy of the interaction of co-assembly with cells

While the fluorescent level of the peptide was measured after incubation with cells by flow cytometry, we sought more information about the location of the Rho-peptide, Cy3-DNA, and the co-assembly with respect to the cells by confocal microscopy. The co-assembly used for confocal microscopy study contained 1:2 tagged: untagged DNA (**Figure 6d**). After resuspending the sonicated samples (Rho-peptide, Cy3-DNA, and co-assembly) in 1X PBS, the morphologies were confirmed by TEM. Cy3-DNA alone stably entered the cells and associated with nucleus after 0.5 h of incubation (**Figure 9a**). It also remained in the cytoplasm for at least 4 h (**Figure 9f**). Meanwhile, Rho-peptide did not enter the cytoplasm at either time point (**Figure 9b**, **Figure 9g**). When the cells were treated with the co-assembly, however, we first noticed the co-localization of the two biopolymers because the locations of the two fluorophores were identical (**Figure 9c-e, h-j**). After 4 hours of incubation, co-localization persisted (**Figure 9h-j)**, suggesting the stability of the co-assembly with cells. For future experiments, later time points should also be included to test the stability of the co-assembly in cellular environment.

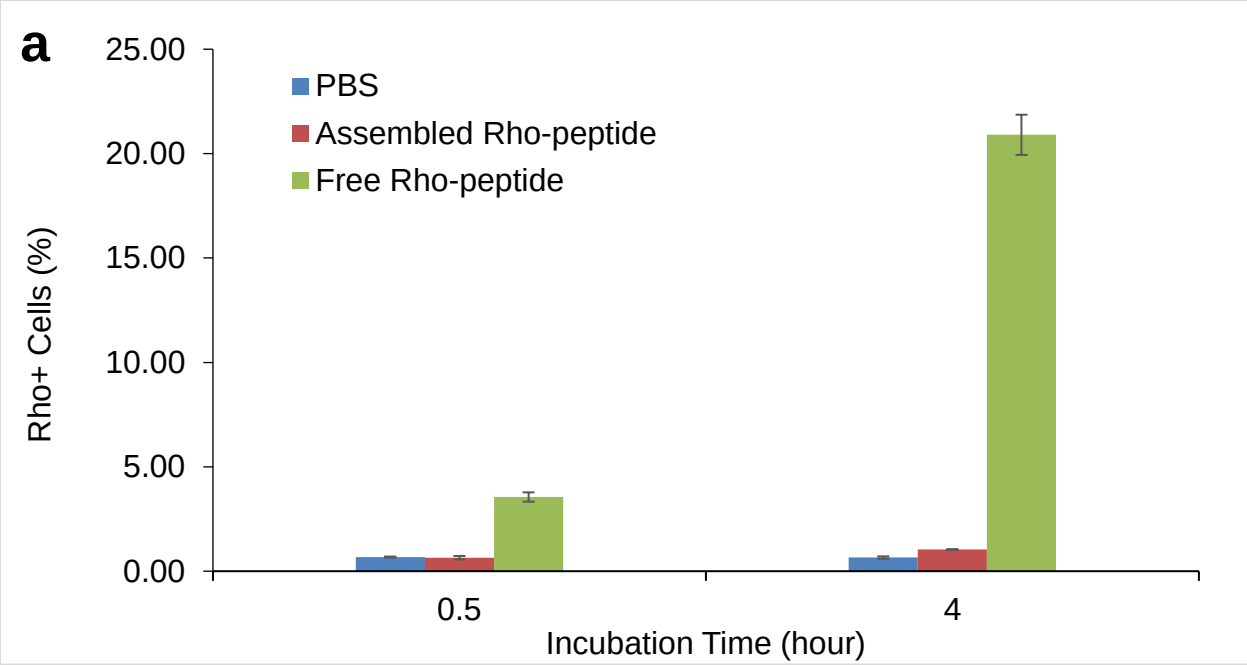

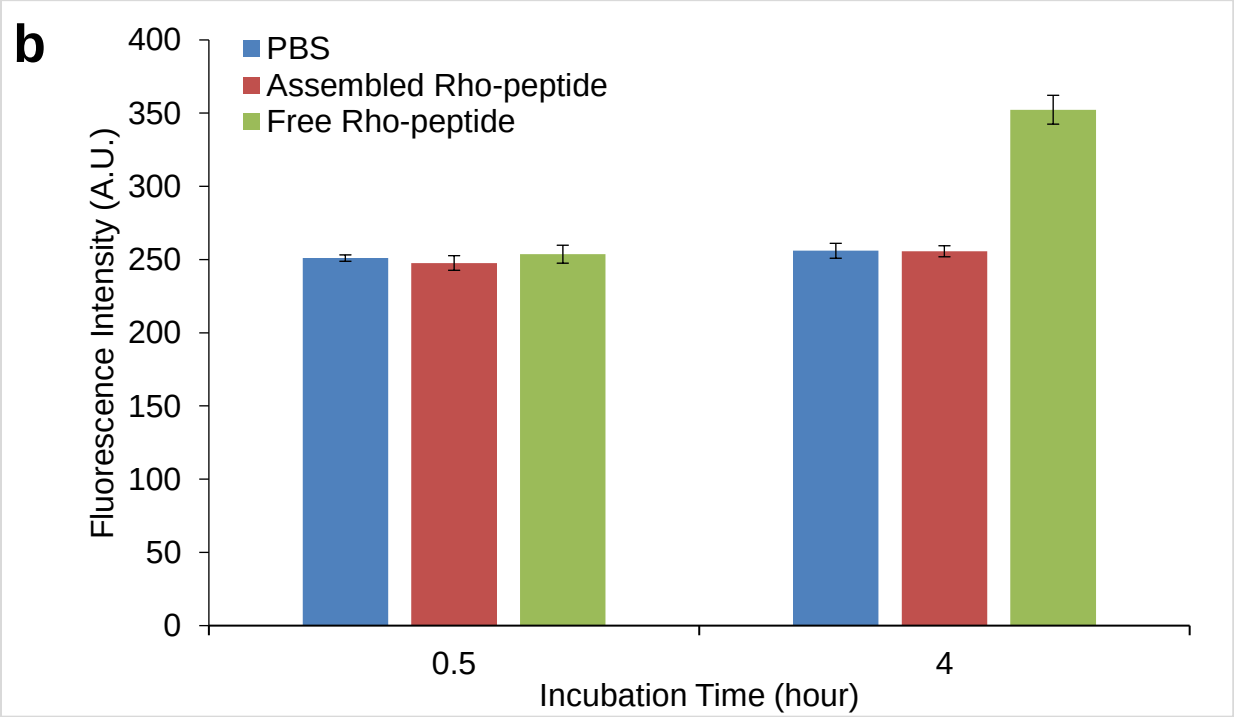

Figure 8. Cellular association of sonicated, assembled Rho-peptide and unassembled Rho-KLVIIAG-NH_2 in comparison with 1XPBS as treatment control by flow cytometry. a) Average percentage of rhodamine-positive cells from 3 replicates after 0.5 and 4 h of incubation with treatments. Error bars represent standard deviation. b) The average fluorescene intensity of the rhodamine-positive cells from 3 replicates after 0.5 and 4 h of incubation with treatments. Error bars represent standard deviation.

The confocal images did not provide enough detail and resolution to examine the level of internalization. The co-assembly appears to be attached to cell surface based on the confocal images (**Figure 9**), but without a membrane marker, it was difficult to distinguish co-assembly that was not washed off from the slides and samples that attached to cell surface. Nevertheless, it was evident that the co-assembly behaved very differently with cells when compared with its independent biopolymer components (**Figure 9**). To further dissect whether cellular uptake occurs, future experiments should utilize flow cytometry to quantify the fluorescent level, and perform Western blots with an antibody for the peptide component following cell lysis. In terms of identifying the location of the co-assembly, it will also be beneficial to use membrane and other subcellular markers. Different cell lines with various levels of phagocyticity should also be tested. To access the possibility of nucleic acid facilitating Aβ peptide internalization in AD, measuring association and uptake level in neuron cell assay will be particularly critical. Importantly, the co-assembly employed in this incubation study matured into bundled fibers (**Figure 6d**), even though we intended to assemble tubes which has higher stability and provides a platform for further modification. After the system is optimized to achieve uniform tubular morphologies, it would be necessary to repeat this experiment.

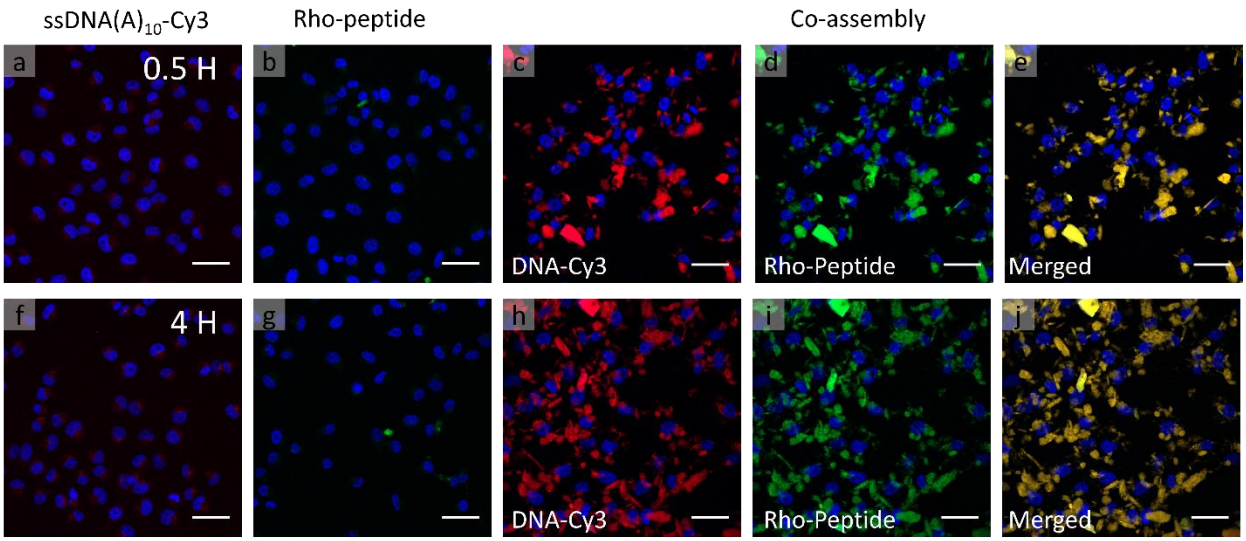

Figure 9. The cellular internalization of Cy3-tagged DNA, Rho-peptide, and co-assembly (Rho-peptide and 1:2 tagged:untagged DNA) was examined by confocal microscopy at 40x magnification after 0.5 hour (first row) and 4 hours (second row) of incubation with H1299 non-small lung cancer cell line. a, f) ssDNA$(A)_{10}$-Cy3 incubated with cells for 0.5 hour and 4 hours, respectively, demonstrating internalization in the cytoplasm. b, g) Rho-peptide incubated with cells for 0.5 hour and 4 hours, respectively. There is no internalization of Rho-peptide assemblies. c-e, h-j) Co-assemblies incubated with cells for 0.5 hour and 4 hours, respectively. Merged channels showed colocalization of Rho-peptide and DNA. Blue = nuclei of the non-small lung cancer cells; green = Rho-peptide; red = ssDNA$(A)_{10}$-Cy3.

Conclusion

For the construction of a fluorescent inside-out virus using Aβ peptide and nucleic acid, the previously synthesized peptide, KLVIIAG, was conjugated with rhodamine 110 and ssDNA was conjugated with Cy3. With the attachment of fluorophores, the peptide and DNA assembled into both tubes and fibers that were stable in 1X PBS. To promote a more homogenous system with only tubular structures, different ratios of tagged to untagged nucleic acid were utilized in the co-assembly with un-desalted peptides. While ribbons emerged during maturation of the co-assemblies, only bundled fibers were observed after 36 days of incubation, suggesting the effect of mixed DNA on the formation of nanotubes. The system can be further optimized by mutating the peptide sequence and using alternative fluorophores. Furthermore, cellular association of the assembled Rho-peptide examined by flow cytometry showed that there was no significant association of sonicated peptides, but unassembled Rho-KLVIIAG-NH_2 stably associated with cells as indicated by increase percentage of rhodamine-positive cells and mean fluorescence level. To determine the location of co-assembly with respect to cells, confocal microscopy was utilized for visualization. While DNA alone effectively associate with the nucleus, peptide-assembled fibers did not. For the co-assemblies, they remained intact when incubated with cells and preliminary experiments found them to be either attached to the cell surface, internalized or both. The images were not sufficiently conclusive to determine whether cellular uptake occurred, so further experiments will be needed to quantify the intracellular co-assemblies, if any. Subcellular and membrane markers will also be useful in visualizing the location of co-assemblies with better confidence. After optimization of the system to yield co-assembling peptide-DNA nanotubes is completed, cellular uptake studies using different cell lines can be explored. Overall, these studies have laid the foundation for the study of an inside-out virus with

fluorescent peptide-DNA co-assemblies, and successfully assessed preliminary results on the cellular association performance of these unique structures.

Materials and Methods

Peptide synthesis

Peptides were synthesized using a solid state peptide synthesis (SPPS) protocol with a Liberty CEM Microwave Automated Peptide Synthesizer (Matthews, NC, USA) with Rink-Amide MBHA resin, 0.4mmol/g substitution. All peptides, except for rhodamine-tagged KLVIIAG-NH_2, were capped with an acetyl group at the N-terminus. Cleavage of peptide off the solid support was achieved by using a cocktail of 95% trifluoroacetic acid (TFA), 5% thioanisole, 3% 1,2-ethanediethiol, and 2% anisole. The cleavage product was then precipitated in -20 ˚C diethyl ether. After washing with diethyl ether 3 times, the crude peptides were centrifuged and dried in a vacuum desiccator for 3 days. The cleavage product was further purified by reverse-phase HPLC with 0.1% TFA + acetonitrile and 0.1% TFA + water as mobile phase and a C18 column. After removing acetonitrile and TFA via rotavaporation, the purified aqueous solution was flash frozen with liquid nitrogen and lyophilized to afford a white powder for storage. The composition of the peptide was confirmed with MALDI mass spectrometry with α-cyano-4-hydroxycinnamic acid (CHCA) matrix.

Rhodamine-tagged peptide preparation

Uncapped KLVIIAG-NH_2 attached on the resin was allowed to swell in 1-2 mL of anhydrous dimethylformamide (DMF) for 30 min before rhodamine conjugation. To activate the carbonyl group on the rhodamine 110 (75% dye content), O-(7-Azabenzotriazole-1-yl)-N,N,N,N'-tetramethyluronium hexafluorophosphate (HATU) was mixed with rhodamine 110 in 1mL of anhydrous DMF for 10 mins at room temperature with stirring. The activated rhodamine solution was then transferred to the KLVIIAG-NH_2 resin and stirred for 20 min. Amine activator diisopropylethylamine (DIEA) was subsequently added to the reaction mixture. The reaction was

stirred for 16 hours in the dark and under nitrogen gas. After the reaction completed, the rhodamine-conjugated peptide resins were isolated by vacuum filtration and washed with 200 mL dimethyl sulfoxide (DMSO)/DMF twice, 200 mL DMF twice, and 200 mL dichloromethane (DCM) twice before drying in a desiccator. Subsequent cleavage and purification follows standard protocol as indicated previously.

Desalting and disaggregation

When noted, certain peptides were desalted using Sep-Pak C18 Classic cartridges. The cartridge was first activated by pushing the following solvents through the cartridge with a syringe: 9mL of acetonitrile, 3mL of 50% acetonitrile in water, and 3mL of 0.5% acetic acid in water. Activation was followed by equilibration with 9mL of pure water. Sample dissolved in 1 mL of 40% acetonitrile was then syringed through the cartridge at a rate of 1 drop/second. To desalt the peptide, 9mL of pure water was slowly pushed through the cartridge. The desalted peptide was finally eluted with 5mL of 50% acetonitrile + 0.5% acetic acid in water. Organic solvent was removed from the peptide solution by rotavaporation before lyophilization. Lyophilized peptide was stored in -20 ˚C until assembly. For disaggregation, peptides were dissolved in minimum volume of HFIP, then the solvent was evaporated by a CentriVap Benchtop Vacuum Concentrator at 40 ˚C for 15 mins.

Peptide assembly and peptide/nucleic acid co-assembly

Stock solution of 8μM Rho-KLVIIAG-NH_2 was prepared in 40% acetonitrile. To prepare a stock peptide solution of 8μM:2mM Rho-KLVIIAG-NH_2: Ac-KLVIIAG-NH_2 in 40% acetonitrile, 8μM Rho-KLVIIAG-NH_2 was prepared, then appropriate amount of untagged peptide was dissolved in this 8uM tagged-peptide solution to achieve 2mM concentration. pH was not

adjusted. Final peptide assembly concentration was 4μM:1mM Rho-KLVIIAG-NH_2: Ac-KLVIIAG-NH_2.

For the peptide/nucleic acid co-assembly, all nucleic acids were purchased from Integrated DNA Technologies. Single-stranded DNA was used throughout all experiments and the nucleic acid sequence used for the co-assembly was 5'AAA AAA AAA A 3'. Cy3 were conjugated to the 3' terminal of the poly-A sequence. A stock solution of 1 mM untagged nucleic acid was prepared. Stock fluorescent peptide was prepared as described above. The order of addition was peptide, solvent, and then nucleic acid. Final peptide and nucleic acid concentration was at 1:1 charge ratio (i.e. 1 mM peptide with 0.1 mM poly$(A)_{10}$).

For experiments with altered tagged and untagged DNA ratio, a 2 mM stock solution of untagged DNA and a 1 mM stock solution of tagged DNA were prepared. A solution of untagged and tagged nucleic acid mixture was then prepared at 1 mM concentration with respect to untagged DNA. Fluorescent peptide stock solution was prepared as described previously. Then the co-assembly was achieved by adding the appropriate amount of peptide, solvent, then nucleic acid within 5 minutes.

All samples were assembled in 40% acetonitrile at 37˚C, unless specified. Two replicates were assembled for each condition.

Transmission electron microcopy (TEM)

Electron micrographs were obtained using a Hitachi H-7500 transmission electron microscopy, operating at 80kV. For sample preparation, 8 μL of sample solution was placed on CF200-Cu carbon film 200 mesh copper grid, allowed to settle for 1 min, then excess solution was wicked away by filter paper. About 8 μL of 1% uranyl acetate was then placed on the same grid for 1

min for negative staining. Similarly, excess staining solution was wicked away by filter paper. The grid with stained samples was stored in vacuum desiccator overnight before TEM analysis.

Fourier Transform Infrared (FT-IR) Spectroscopy

A Jasco FT-IR 4100 (Easton, MD, USA) was utilized to acquire all spectra averaging 800 scans at 2 cm^{-1} resolution. After taking a background scan, 8 μL of sample was dried on a Pike GaldiATR (Madison, WI, USA) ATR diamond. Sample scans were then acquired after subtracting the background.

Sonication, and resuspension of assembly in PBS

For sonication, the sonication probe was placed into the sample without touching the tube. Samples were sonicated continuously for 30 seconds with an amplitude of 30%. For resuspension of assembly, sample was first centrifuged at 22 ˚C for 1-2 hours until a pellet is formed. Supernatant is removed from the pellet and equivalent volume of 1xPBS was added. Sample in PBS is resuspended by vortex for a few minutes.

Cell incubation and flow Cytometry

H1299 (Non Small Cell Lung Cancer Cell line) was used for the incubation study. After 60,000 cells/well in 24-well plates were seeded, they were incubated at 37 ˚C overnight for cells to settle down, and samples (250 nM of fluorescent component) in 250 μL final volume with different time points (30 mins and 4 hours) were treated. After treatment, the cells were washed with 1X PBS for 1 min, 3 times, then they were suspended with 0.25% trypsin. Cell suspension was centrifuged at 5000 rpm for 5 minutes. Supernatants were discarded. Sediments were washed with 1X PBS, then it was centrifuged again at 5000 rpm for 5 minutes. After discarding the supernatant, the cells were suspended with 400 μL of 1X PBS for flow cytometry analysis. Three replicates were made for each sample condition. Flow cytometry determined percentage of

Rhodamin-110 and intensity of dye conjugated with peptide. All data was analyzed by FlowJo Software.

Cell fixing and confocal microscopy

After incubation of certain time period, treated cells were fixed on slides using 4% paraformaldehyde for 30 mins at room temperature, washed with 1X PBS 3 times, and DAPI was applied for nuclear staining. Coverslips were sealed with clear nail polish. Fluorescence micrographs were acquired by an Olympus FV1000 laser-scanning confocal microscope using 40X 1.30NA oil immersion objective. The 405 nm, 448nm, and 488 laser lines were used to visualize DAPI nuclear staining, rhodamine 110, and Cy3, respectively. All images were processed using Fiji.

References

1. Robertson, M. P.; Joyce, G. F., The Origins of the RNA World. *Cold Spring Harb. Perspect. Biol.* **2012,** *4* (5), a003608.

2. Kruger, K.; Grabowski, P. J.; Zaug, A. J.; Sands, J.; Gottschling, D. E.; Cech, T. R., Self-splicing RNA: Autoexcision and autocyclization of the ribosomal RNA intervening sequence of tetrahymena. *Cell* **1982,** *31* (1), 147-157.

3. Cech, T. R., The Ribosome Is a Ribozyme. *Science* **2000,** *289* (5481), 878.

4. Petrov, A. S.; Gulen, B.; Norris, A. M.; Kovacs, N. A.; Bernier, C. R.; Lanier, K. A.; Fox, G. E.; Harvey, S. C.; Wartell, R. M.; Hud, N. V.; Williams, L. D., History of the ribosome and the origin of translation. *Proceedings of the National Academy of Sciences* **2015,** *112* (50), 15396.

5. Chernoff, Y. O., Amyloidogenic domains, prions and structural inheritance: rudiments of early life or recent acquisition? *Curr. Opin. Chem. Biol.* **2004,** *8* (6), 665-671.

6. Li, J.; Browning, S.; Mahal, S. P.; Oelschlegel, A. M.; Weissmann, C., Darwinian Evolution of Prions in Cell Culture. *Science* **2010,** *327* (5967), 869.

7. Liebman, S. W.; Chernoff, Y. O., Prions in yeast. *Genetics* **2012,** *191* (4), 1041-72.

8. Petty, S. A.; Adalsteinsson, T.; Decatur, S. M., Correlations among Morphology, β-Sheet Stability, and Molecular Structure in Prion Peptide Aggregates. *Biochemistry* **2005,** *44* (12), 4720-4726.

9. King, C.-Y.; Diaz-Avalos, R., Protein-only transmission of three yeast prion strains. *Nature* **2004,** *428*, 319.

10. Laurent, M., Prion diseases and the 'protein only' hypothesis: a theoretical dynamic study. *Biochem. J.* **1996,** *318* (Pt 1), 35-39.

11. Ma, J.; Wang, F., Prion disease and the 'protein-only hypothesis'. *Essays Biochem.* **2014,** *56*, 181.

12. Macedo, B.; Millen, T. A.; Braga, C. A.; Gomes, M. P.; Ferreira, P. S.; Kraineva, J.; Winter, R.; Silva, J. L.; Cordeiro, Y., Nonspecific prion protein-nucleic acid interactions lead to different aggregates and cytotoxic species. *Biochemistry* **2012,** *51* (27), 5402-13.

13. Silva, J. L.; Cordeiro, Y., The "Jekyll and Hyde" Actions of Nucleic Acids on the Prion-like Aggregation of Proteins. *J Biol Chem* **2016,** *291* (30), 15482-90.

14. Deleault, N. R.; Lucassen, R. W.; Supattapone, S., RNA molecules stimulate prion protein conversion. *Nature* **2003,** *425*, 717.

15. Mehta, A. K.; Rosen, R. F.; Childers, W. S.; Gehman, J. D.; Walker, L. C.; Lynn, D. G., Context dependence of protein misfolding and structural strains in neurodegenerative diseases. *Biopolymers* **2013,** *100* (6), 722-30.

16. Childers, W. S.; Anthony, N. R.; Mehta, A. K.; Berland, K. M.; Lynn, D. G., Phase networks of cross-beta peptide assemblies. *Langmuir* **2012,** *28* (15), 6386-95.

17. Braun, S.; Humphreys, C.; Fraser, E.; Brancale, A.; Bochtler, M.; Dale, T. C., Amyloid-Associated Nucleic Acid Hybridisation. *PLoS One* **2011,** *6* (5), e19125.

18. Taran, O.; Chen, C.; Omosun, T. O.; Hsieh, M.-C.; Rha, A.; Goodwin, J. T.; Mehta, A. K.; Grover, M. A.; Lynn, D. G., Expanding the informational chemistries of life: peptide/RNA networks. *Philosophical Transactions of the Royal Society A: Mathematical, Physical and Engineering Sciences* **2017,** *375* (2109).

19. Rahman Mohammad, A.; Wang, P.; Zhao, Z.; Wang, D.; Nannapaneni, S.; Zhang, C.; Chen, Z.; Griffith Christopher, C.; Hurwitz Selwyn, J.; Chen Zhuo, G.; Ke, Y.; Shin Dong, M.,

Systemic Delivery of Bc12-Targeting siRNA by DNA Nanoparticles Suppresses Cancer Cell Growth. *Angew. Chem. Int. Ed.* **2017,** *56* (50), 16023-16027.

20. Wang, P.; Rahman, M. A.; Zhao, Z.; Weiss, K.; Zhang, C.; Chen, Z.; Hurwitz, S. J.; Chen, Z. G.; Shin, D. M.; Ke, Y., Visualization of the Cellular Uptake and Trafficking of DNA Origami Nanostructures in Cancer Cells. *J. Am. Chem. Soc.* **2018,** *140* (7), 2478-2484.

21. Ow, S. Y.; Dunstan, D. E., A brief overview of amyloids and Alzheimer's disease. *Protein Sci* **2014,** *23* (10), 1315-31.

22. Ghiso, J.; Frangione, B., Amyloidosis and Alzheimer's disease. *Adv. Drug Del. Rev.* **2002,** *54* (12), 1539-1551.

23. Burkoth, T. S.; Benzinger, T. L. S.; Urban, V.; Morgan, D. M.; Gregory, D. M.; Thiyagarajan, P.; Botto, R. E.; Meredith, S. C.; Lynn, D. G., Structure of the β-Amyloid(10-35) Fibril. *J. Am. Chem. Soc.* **2000,** *122* (33), 7883-7889.

24. Uversky, V. N.; Fink, A. L., Conformational constraints for amyloid fibrillation: the importance of being unfolded. *Biochim. Biophys. Acta* **2004,** *1698* (2), 131-153.

25. Smith Jillian, E.; Liang, C.; Tseng, M.; Li, N.; Li, S.; Mowles Allisandra, K.; Mehta Anil, K.; Lynn David, G., Defining the Dynamic Conformational Networks of Cross-β Peptide Assembly. *Isr. J. Chem.* **2015,** *55* (6-7), 763-769.

26. Omosun, T. O.; Hsieh, M.-C.; Childers, W. S.; Das, D.; Mehta, A. K.; Anthony, N. R.; Pan, T.; Grover, M. A.; Berland, K. M.; Lynn, D. G., Catalytic diversity in self-propagating peptide assemblies. *Nat. Chem.* **2017,** *9*, 805.

27. Rengifo, R. F.; Li, N. X.; Sementilli, A.; Lynn, D. G., Amyloid scaffolds as alternative chlorosomes. *Org. Biomol. Chem.* **2017,** *15* (34), 7063-7071.

28. Li, S.; Mehta, A. K.; Sidorov, A. N.; Orlando, T. M.; Jiang, Z.; Anthony, N. R.; Lynn, D. G., Design of Asymmetric Peptide Bilayer Membranes. *J Am Chem Soc* **2016,** *138* (10), 3579-86.

29. Liang, Y.; Lynn, D. G.; Berland, K. M., Direct Observation of Nucleation and Growth in Amyloid Self-Assembly. *J. Am. Chem. Soc.* **2010,** *132* (18), 6306-6308.